Fabrication of Mixed Matrix Hollow Fibers with Intimate Polymer–Zeolite Interface for Gas Separation

Lan Ying Jiang and Tai Shung Chung
Dept. of Chemical and Biomolecular Engineering, National University of Singapore, Singapore 119260

Santi Kulprathipanja
UOP LLC, Des Plaines, IL 60017

DOI 10.1002/aic.10909
Published online June 8, 2006 in Wiley InterScience (www.interscience.wiley.com).

It has been demonstrated that a novel p-xylenediamine/methanol soaking method could efficiently remove the polymer–zeolite interface defects of the mixed-matrix structure. In this work, the mixed-matrix structure is in the form of an ultrathin (1.5–3 μm) polysulfone/zeolite beta mixed-matrix layer that is supported by a neat Matrimid® layer in dual-layer composite hollow fibers. The particle's loading in this thin layer has reached 30 wt %. The ideal selectivities of the mixed-matrix hollow fibers (30 wt % of zeolite) for O_2/N_2 and CO_2/CH_4 separation were roughly 30 and 50% superior to that of the neat PSF/Matrimid® hollow fibers, respectively. Investigation of the morphology of the mixed-matrix selective layer and its relation with gas separation performance indicated that without p-xylenediamine/methanol solution treatment, the outer layer showed various polymer–zeolite interface structures in different fibers with the same heat treatment procedures; this situation might lead to the different selectivities after coating. However, by applying p-xylenediamine/methanol processing on the fibers before thermal treatment, the fibers obtained a more uniform structure and improved attachment between polymer matrix and zeolite surface. Hydrogen bonding was proposed as the possible mechanism for the tighter attachment between the two phases. The improvement of separation efficiency was presumably related to the polymer chain rigidification, partial pore blockage, and/or favorable interaction between the gas penetrants and zeolite framework.
 AIChE J, 52: 2898–2908, 2006
Keywords: dual-layer hollow fibers; mixed-matrix composite skin; zeolite beta; p-xylenediamine/methanol treatment; heat treatment

Introduction

Nowadays, hollow fibers constitute a preferred membrane configuration for many separation processes. This is mainly attributed to its thin selective layer, high surface area per unit volume, good flexibility, and easy module fabrication.[1,2] To achieve higher efficiency in separation, various efforts have been made in developing materials with superior properties into hollow fibers. Among the novel materials, mixed-matrix membranes (MMMs)—consisting of polymers and zeolites,[3] polymers and carbon molecular sieves (CMS),[4] polymer and nanoparticles,[5] and CMS and zeolites[6]—are gaining significant interest, particularly in gas separation and pervaporation. The separation process in inorganic materials is based on either the size and shape or the sorption-selective nature of those materials. These inorganic materials generally have higher selectivity than that of polymeric membranes in various separation processes.[3-9] Thus, the addition of inorganic domains into a

Correspondence concerning this article should be addressed to T. S. Chung at chencts@nus.edu.sg.

polymer matrix is expected to improve the separation factor of polymeric membranes, without compromising membrane flexibility.

Most research on mixed-matrix membranes (MMMs) has primarily focused on the forms of flat dense and asymmetric films of which the properties and advantages have been discussed in extensive detail.[10-37] For instance, Paul and Kemp discovered a delayed diffusional time lag effect for CO_2 and CH_4 when zeolite 5A particles were added into polydimethylsiloxane (PDMS).[15] Later, Kulprathipanja et al.[3,17] reported that O_2/N_2 selectivity improved from 3.0 to 4.3 by dispersing silicalite (20 wt % loading) into cellulose acetate. For an intense application environment, as seen in gas separation, membranes with polymers of high glass-transition temperature (T_g) values are more favored than rubbery polymers, despite the ease in forming MMMs with the latter. However, there are many questions and problems associated with this strategy for making more selective membranes. Removing voids at the particle–polymer interface is a central one. Extensive and intensive works have been carried out to promote adhesion between the rigid polymer chains and molecular sieves. These works include thermal treatment, silane coupling agents, integral chain linkers, and polymer coating on the molecular sieve surface.[4,19-21,23,24,31,34] For example, by applying thermal treatment at high temperatures, Rojey et al.[23] obtained selectivity enhancement for H_2/CH_4 gas mixtures using MMMs consisting of zeolite 4A and the Ultem® matrix. In a published patent Kulkarni et al.[24] reported that MMMs with silane-modified zeolite H-SSZ-13 dispersed in the Ultem® matrix exhibited selectivity of 10.4 to 10.8 for O_2/N_2 separation (the selectivity of neat Ultem® for O_2/N_2 separation is 7.8). For Matrimid®–zeolite MMMs, Yong et al.[31] introduced a compatibilizer 2,4,6-triaminopyrimidine (TAP). It was postulated that hydrogen bonding induced between TAP and 4A as well as TAP and Matrimid® helped form a void-free membrane. Results showed that CO_2/N_2 and O_2/N_2 selectivity of Matrimid®–4A–TAP membranes increased by around threefold compared with pure Matrimid® membranes. Boom[19] proposed coating of zeolite particles in dilute solutions with a monolayer of polymer, although no experiments were reported. Vu et al.[4] fabricated MMMs with a rigid polyimide, Matrimid® 5218 (T_g = 302°C), and CMS particles. By applying the technique of polymer coating on the CMS surface, the interface defects were efficiently removed and the resultant MMMs had improved permeability as well as selectivity for O_2/N_2 and CO_2/CH_4 separation.

In some studies, the molecular sieving effect of inorganic domains was suggested as the major cause for the increment in perselectivities. Mahajan[29] found that the superior entropic discrimination between O_2 and N_2 in zeolite 4A led to the selectivity of O_2/N_2 for 4A-Ultem® MMMs being almost double what it was for neat Ultem® membranes. In the study reported by Duval,[20] however, an increase of CO_2/CH_4 selectivity from 13.5 to 35 with a MMM containing 46 vol % zeolite KY in NBR was attributed to the affinity of the gas molecules for the zeolite internal surface. In a recent research work Anson et al.[35] observed that incorporation of activated carbon into acrylonitrile–butadiene–styrene (ABS) terpolymer (0.624 volume fraction) significantly improved CO_2/CH_4 selectivity from 24.1 to 50.5. The results were partially explained by the preferential surface diffusion of CO_2 gas (more adsorbable gas) over the CH_4 gas (less adsorbable gas).

As we can see from previous work, MMM is clearly an attractive alternative to neat polymeric membranes. However, how to possibly convert mixed-matrix materials into hollow fibers with high permeance and high selectivity has received a great deal of attention, yet the research in this area is quite limited. Except for our recent works,[38-40] the process of fabricating hollow fibers with a mixed-matrix selective layer can be found only in patents with limited scientific teaching.[41-43] With this primary objective in mind, a series of investigations focused on the fabrication of dual-layer hollow fibers with a polymer/zeolite mixed-matrix outer sheath was carried out.

In this particular work, the polymer used for the continuous phase of the outer selective layer was polysulfone (PSF); a self-synthesized zeolite beta with an average particle size of around 0.4 μm was used as the dispersed phase; Matrimid® 5218 was chosen as the inner support layer material because of its excellent thermal and mechanical properties. Double-layered hollow fibers[44-47] were applied here mainly for two reasons: (1) it can reduce material cost because it requires only one of the two materials to be deemed expensive and of high performance as the selective layer; (2) the two polymers chosen for the outer and inner layers have a vast gap in glass-transition temperatures, here PSF (T_g = 185°C) vs. Matrimid® (T_g = 302°C), which makes the posttreatment aimed at the selective outer layer containing PSF, possibly with the least densification effect on the Matrimid® inner layer. To overcome this challenging issue of interface defects in inorganic/organic mixed-matrix membranes, a novel approach of *p*-xylenediamine/methanol solution soaking was proposed as a supplementary method of thermal annealing and surface coating to yield a defect-free mixed-matrix structure more efficiently. The primary goal is to fully exploit the separation property of zeolites.

Experimental

Materials

Udel® polysulfone (PSF) from Amoco and Matrimid® 5218 from Vantico were the polymers used in this study; polymers were dried at 110–120°C under vacuum overnight before dope preparation. *N*-Methyl-pyrrolidinone (NMP) and ethanol (EtOH) from Merck were used as the solvent and nonsolvent, respectively. Zeolite beta particles synthesized in our lab were added to the spinning solution for the mixed-matrix outer layer of dual-layer hollow fibers; the particles had an average diameter of about 0.4 μm. All the particles were dehydrated at 350°C for 2 h under vacuum before being immediately immersed into dehydrated NMP; *p*-xylenediamine, and methanol for treating hollow fibers were purchased from Tokyo Chem and Merck, respectively.

Hollow fiber fabrication

Dope Preparation. Preparation of the homogeneous Matrimid® solutions were based on methods reported elsewhere.[45] For the heterogeneous polymer solution containing particles, some modifications were made. First of all, the particles were dispersed into NMP and the mixture was stirred for 1 day at a high speed of about 400–500 rpm. This particular step forced the particles to become discrete at high shear rates.

Table 1. Dope Compositions for the Dual-Layer Mixed-Matrix Hollow Fibers

Layer	Polymer	Solvent		Polymer Concentration (wt %)	Molecular Sieves**	
		Composition	Ratio		Type	Loading in Polymer (wt %)
OL0	PSF	NMP	—	37	—	—
OL1	PSF	NMP	—	30	Beta	10
OL2	PSF	NMP	—	30	Beta	20
OL3	PSF	NMP	—	30	Beta	30
IL	Matrimid®	NMP/EtOH	4/1	23	—	—
Bore	—	NMP/H_2O	95/5	—	—	—

OL is outer layer; IL is inner layer.
**The particles were synthesized by Dr. Huang Zhen.

Other steps were the same as those of homogeneous solutions. Before spinning, the homogeneous solution was first degassed in the stirring flask for 24 h; upon completion, the solution was put into the pump for another 24 h and degassed, although the heterogeneous dope was removed to the pump right after stirring and then vacuum degassed for only 2 h. Table 1 shows the compositions of dopes for dual-layer hollow fibers. The zeolite loading is expressed in weight percent (wt %) by the following equation:

$$100 \times \text{weight of zeolite}/(\text{weight of zeolite} + \text{weight of polymer})$$

The polymer solutions used for obtaining the outer layer and inner layer were referred to as OL and IL, respectively. The high polymer concentration in the mixed-matrix layer is vital because it prevents particles from sedimentation in the dope. To form a more porous substrate structure, the Matrimid® concentration in the inner layer dope was chosen to be 23 wt %. EtOH was added as the nonsolvent in the inner layer to increase bulk porosity in the substrate layer.[45]

Hollow-Fiber Spinning. Dual-layer hollow fibers were spun according to the procedure described elsewhere.[45-47] Details of spinning conditions and parameters are summarized in Table 2. By lowering the outer layer flow rate (while keeping other spinning conditions constant), the thickness of the outer layer can be reduced.[39] The as-spun fibers were rolled up by a drum and then cut into segments before being rinsed in a clean water bath for at least 5 days to remove the remaining NMP. Solvent exchange was then carried out by first soaking the fibers in methanol (three times, each session 30 min), then repeating the same procedure but this time with *n*-hexane. After being removed from the hexane, the fibers were air-dried at room temperature.

Table 2. Spinning Parameters for the Dual-Layer Mixed-Matrix Hollow Fibers

Spinning Parameter	Fiber ID Values			
	DLA	DLB	DLC	DLD
Flow rate (cm^3/min)				
Outer layer	0.12	0.8	0.6	0.8
Inner layer		0.8		0.8
Bore fluid		0.3		0.3
Air gap (cm)		0.0		6.0
Take-up rate (m/min)		Free draw		
Temperature (°C)				
Coagulant		25		
Spinneret		25		

Posttreatment of as-spun hollow fibers and coating

Posttreatment that combined both chemical and thermal approaches was implemented to improve the hollow-fiber separation performance. The flow chart of posttreatment and coating procedures is shown in Figure 1. Initially, the as-spun fibers after solvent exchange were immersed in the *p*-xylenediamine/methanol solution (2.5/100 w/v) for 1 h; thereafter, the fibers were rinsed in methanol for a few seconds, and then dried on filter paper in air for 1 day; the dried fibers were then annealed at 200°C for 2 h to transform the porous structure of the outer layer into a dense structure.

The fibers processed with these three steps were made into modules and tested according to previous work.[38] Thereafter, they were coated by a two-step method as shown in Figure 1. Each individual step was conducted by dip coating the fiber, while simultaneously applying vacuum to the fiber lumen for 30 min, after which the fibers were annealed at 100°C for 2 h and immediately mounted onto a permeation cell for gas separation test. Diethyltoluenediamine and 1,3,5-benzenetricarbonyl chloride in the two-step process may react with each other to form an amide structure. The network was a result of the reaction that narrowed the gap between the particles and the polymer, thus efficiently trapping the silicon rubber chains. This concept of reactive coating was first proposed by DuPont scientists and later applied on sealing the mixed-matrix membranes.[42,48]

The heat treatment processes were all performed in a precision high-temperature programmable furnace (Centurion ™ Neytech Qex) under vacuum. For comparison, fibers without

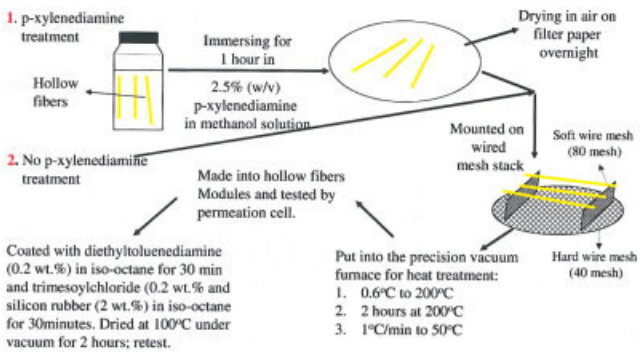

Figure 1. Flow chart of the *p*-xylenediamine/methanol solution soaking, thermal treatment, and coating procedures.

[Color figure can be viewed in the online issue, which is available at www.interscience.wiley.com]

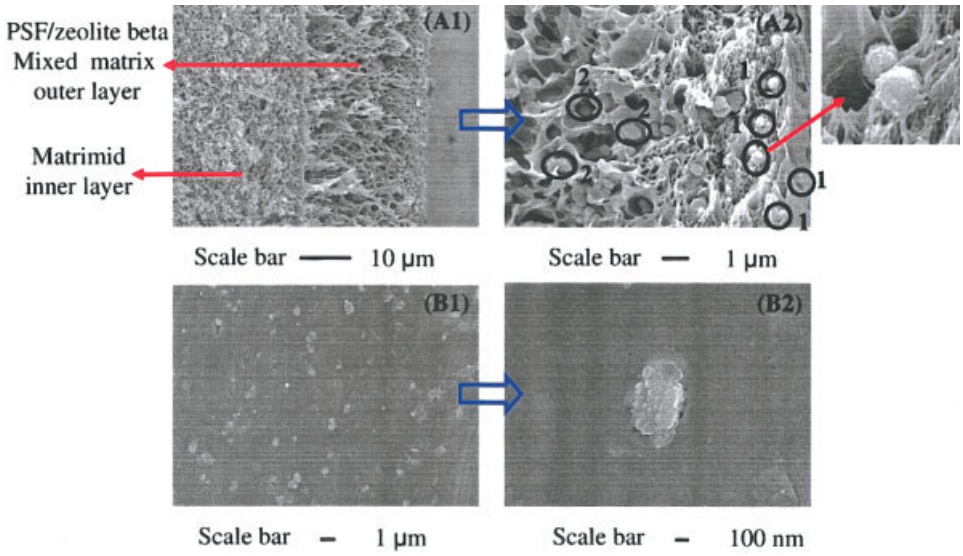

Figure 2. SEM micrographs of the outer layer partial cross section and surface of the as-spun dual-layer hollow fibers (Fiber DL10A).

(A) Cross section; (B) surface. [Color figure can be viewed in the online issue, which is available at www.interscience.wiley.com]

p-xylenediamine/methanol treatment were also thermally treated and coated in exactly the same approach and tested.

Characterization

The morphology of the resulting membranes was observed by using either scanning electron microscopy (SEM, JEOL JSM-5600LV) or field emission scanning electron microscopy (FESEM, JEOL JSM-6700LV). The samples for the SEM characterization were prepared in liquid nitrogen followed by Pt coating.

Gas permeation measurements

The pure gas permeation was measured by a constant volume method as described elsewhere[32] with some modifications deemed suitable for testing hollow fibers. Both the upstream and downstream were evacuated for at least 24 h to remove any gases or vapors sorbed in the membrane. Permeation tests were carried out by introducing the desired gas to the shell side of the hollow fibers. In this study, the testing pressure is 5 atm for all the gases and temperature is 35°C. The permeation rate was calculated from the steady-state pressure increase as a function of time dp/dt (mmHg/s) using the following equation:

$$\frac{P}{l} = \frac{273 \times 10^{10}}{760} \frac{V}{AT\left[\frac{p_0 \times 76}{14.7}\right]} \left[\frac{dp}{dt}\right] \tag{1}$$

in which P is the permeability in Barrer units [1×10^{-10} cm^3(STP)·cm/cm^2·s·cmHg], P/l is the permeance in GPU units (1 GPU = 1×10^{-6} cm^3/cm^2·s·cmHg), l is the thickness of the selective layer (cm), V is the volume of the permeation side (cm^3), p_0 is the feed gas pressure in psia, A refers to the effective separating area of the membrane (cm^2), and T is the operation temperature inside the permeation cell (K). The ideal selectivity of a gas pair A/B is defined as follows:

$$\alpha_{A/B} = \frac{[P/l]_A}{[P/l]_B} \tag{2}$$

Results and Discussion

Morphology of the as-spun hollow fibers

The typical morphology of the as-spun hollow fibers is shown in Figure 2. Figure 2A1 illustrates the cross section including the whole outer mixed-matrix layer and partial inner layer; Figure 2B1 demonstrates a general outer surface morphology. The graphs of the cross section in Figure 2A1 show that both the inner layer and outer layer are porous and the particles in the outer layer are uniformly dispersed in the PSF matrix. Several types of polymer–particle contact can be identified in the cross section shown in Figure 2A2. Within the thin layer (~1 μm thick) at the hollow fiber's outermost surface, the particles indicated by symbol **1** have partial defect-free attachment with the surrounding polymer structure, whereas the remaining portion of the particle is surrounded by obvious interface voids. In the phase-inversion process during hollow-fiber spinning, the outer part of the solution in direct contact with water coagulant may be vitrified instantly; the relatively dense structure formed may tighten around the particles. After solvent exchange, polymer chains may partially pull away from the particle surface as a result of relaxing and shrinking, provided there is no covalent bonding between the organic and inorganic materials. Furthermore, the polymer matrix itself does not form an observable dense layer. Subsequently, a continuous defect-free outer skin cannot be obtained. In the substructure, progressing from the shell side to the bottom side of the outer layer, there is a gradual increase in the size of the pores as shown in Figure 2A2, and the particles located in this part indicated by symbol **2** are almost all entrapped inside the pores or the polymer-lean phase. Figure 2B1 shows that the particles' distribution on the outer surface is homogeneous; nevertheless, in the graph with a higher magnification as shown

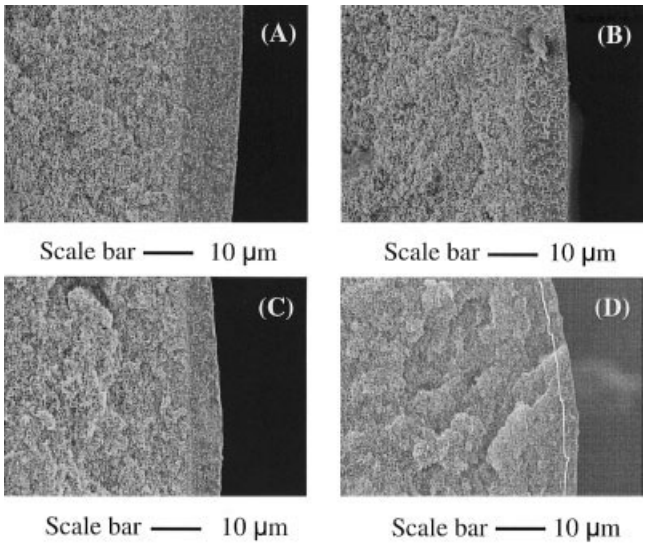

Figure 3. SEM micrographs of the cross-sectional view of the hollow fibers DL3 (20 wt % zeolite loading) after heat treatment at 200°C.

(A) DL3A; (B) DL3B; (C) DL3C; (D) DL3D (referring to the spinning conditions in Table 2).

in Figure 2B2, defects of tens of nanometers were detected at the polymer–zeolite interface. Our previous study[39] clearly revealed that these as-spun fibers had quite low separation property even after coating and heat treatment was a necessary procedure to obtain acceptable performance.

Morphological changes with different posttreatment procedures

Heat treatment is an effective approach to minimize the surface defects and to perfect and densify the selective skins.[49-51] In this study, all the fibers were annealed at 200°C under vacuum according to the procedure shown in Figure 1. Because 200°C is higher than the T_g of PSF, it is expected that the rubber state above PSF's T_g will make the polymer chain quite flexible, thus easily surrounding the particle and decreasing or even removing the various defects. In addition, for phase-separated hollow fibers with mixed-matrix skins encapsulating zeolites, the nonsolvent trapped inside zeolite pores during membrane fabrication and posttreatment may also be more thoroughly removed by heat treatment at high temperatures. Consequently, the zeolites can be really involved in the separation process. The SEM micrographs in Figure 3 show the morphology of the fibers heat treated at 200°C, thus partially confirming the assumptions. The outer layer in Figure 3 is quite dense in contrast with that in Figure 2. Furthermore, the outer layer thickness (ranging from 1.5 to 12 μm) after thermal treatment decreases with either decreasing (lowering) outer layer dope flow rate and/or increasing air gap during spinning.

Effect of Thermal Treatment on the Hollow Fiber Morphology. Figure 4 shows several different morphologies of the cross section observed in the hollow fibers with only heat treatment. The fibers in Figure 4 have an average outer layer thickness of about 1.5 μm. This thickness is about threefold that of the zeolite diameter of 0.4 μm. As a result of the limited spinning conditions applied to the fiber fabrication, the thinner outer layer has not been obtained; therefore, it is premature to make a very confirmative prediction about whether the ratio of

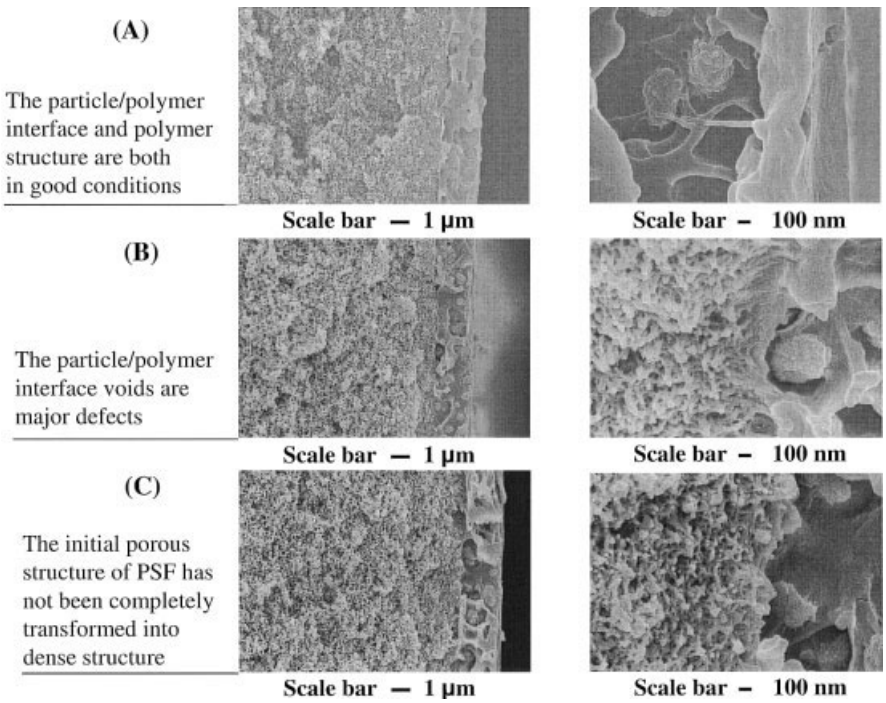

Figure 4. Mixed-matrix outer layer structure of the dual-layer hollow fibers DL3 (20 wt % zeolite loading) without *p*-xylenediamine solution treatment.

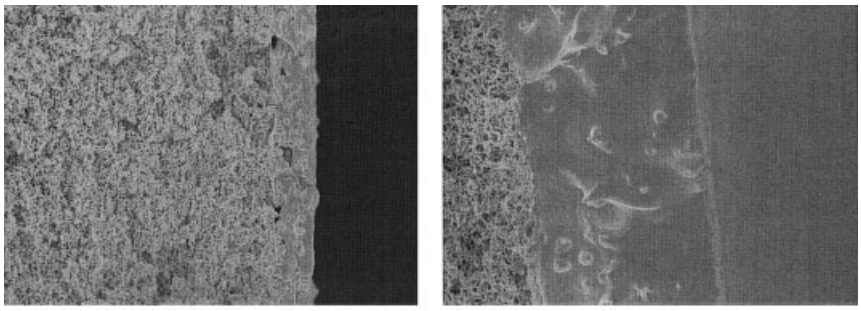

Figure 5. SEM micrographs and separation performance of the dual-layer hollow fibers DL2D (20 wt % zeolite loading) heat treated at 200°C for 6 h.

The graph on right is taken with higher magnification.

outer layer thickness over particle size is always around 3. However, reducing the scales of zeolite and skin layer thickness will be very desirable in improving the productivity.

Even though all the fibers are heat treated with the same procedure, the morphology still exhibits an obvious instability. SEM images in Figure 4A show a well-developed mixed-matrix structure in which the polymer attached tightly to the particles' surface, and the whole outer mixed-matrix layer is homogeneous. It is noticed in Figure 4B that the outer layer is homogeneous; nevertheless, many obvious nanosized polymer–particle interface voids exist. One extreme case is illustrated in Figure 4C of which the outer layer still possesses some large polymer–zeolite interface voids near the inner side, and the whole outer layer is rough. In these three types of morphologies, the one in Figure 4C is least observed. It is known that only when the outer layer is almost homogeneously dense with a defect-free structure (which corresponds to the Figure 4A) can the selectivity of this layer be possibly improved as a result of the mixed-matrix effect.[19] The complicated outer layer structure may give rise to some unpredictable performance of these hollow fibers after coating.

The undesirable morphology in Figure 4B has something in common with the observations in mixed-matrix flat-sheet membrane.[19,20] Even though above T_g heat treatment can aid the polymer chains to surround the zeolite surface more easily, the noncovalent bonding between the two phases probably cannot completely prevent the detachment during annealing. Another factor is that the outer layer is originally porous and most particles just loosely attach to the polymer (Figure 2A2). It is possible that a 2-h period of soaking at 200°C may not be long enough to transform the initially defective outer structure into a fully dense structure; instead, the structure in Figure 4C appears. Another possible cause for the situation in Figures 4B and 4C may be a result of the slightly different hydrophilicities for bulk polymer and zeolite; as a result, the polymer cannot fully wet the particles. To verify whether prolonging the thermal soaking time is effective in attaining a less-defective polymer/zeolite mixed-matrix structure, several fibers are heat treated at 200°C for 6 h; the resulting morphology is shown in Figure 5. Obviously, the large defects on the inner side of the outer layer have been removed; however, the prolonged heat treatment at high temperatures may seriously densify the Matrimid® layer structure and lead to an undesirable resistance to gas transport. The performance of these fibers will be discussed in the next section.

Effect of Combined p-Xylenediamine/Methanol Soaking and Thermal Treatment on Hollow Fiber Morphology. The observation in the previous section implies that in addition to thermal treatment, novel approaches are necessary to compact the polymer and particle contact and make the outer layer structure homogeneous. Priming the sieves with a compatibilizer may be helpful in enhancing the sieves and polymer adhesion. In previous studies, the priming process was carried out either before membrane fabrication (such as silane modification) or by co-mixing the primer within the casting solutions.[4,21,24,34] In this study, the priming process was removed after formation of hollow fibers and solvent exchange. The cross-sectional morphology of hollow fibers with *p*-xylenediamine/methanol soaking and thermal treatment is displayed in Figure 6. The outer layer is strongly attached to the inner layer. Figure 7 shows the outer layer mixed-matrix structure at an even higher magnification for fibers with 30 wt % zeolite loading. Comparison between the fibers (Figure 7A) with and without *p*-xylenediamine solution treatment (Figure 7B) reveals that the former ones have much tighter polymer–zeolite contacts and more homogeneous structure even at zeolite loading of 30 wt %. It is postulated that the $-NH_2$ of the *p*-xylenediamine forms the hydrogen bonding with the –OH groups on the zeolite surface and the sulfonyl oxygen or aryl ether groups in the PSF simultaneously, thus tightening the attachment of the two phases as can be seen in Figure 6. Hydrogen bonding has been advanced by other researchers as one factor leading to the enhanced contact between zeolite and polymer.[31,34] The feasible interaction of *p*-xylenediamine with zeolite and PSF is given in Figure 8. Another observation with these fibers is that the structure of the whole outer layer was completely dense and the morphology in Figure 4C no longer exists. A possible explanation is that the methanol soaking may relax the polymer chains that may be conducive to the polymer adhesion to the zeolite surface during heat treatment. In addi-

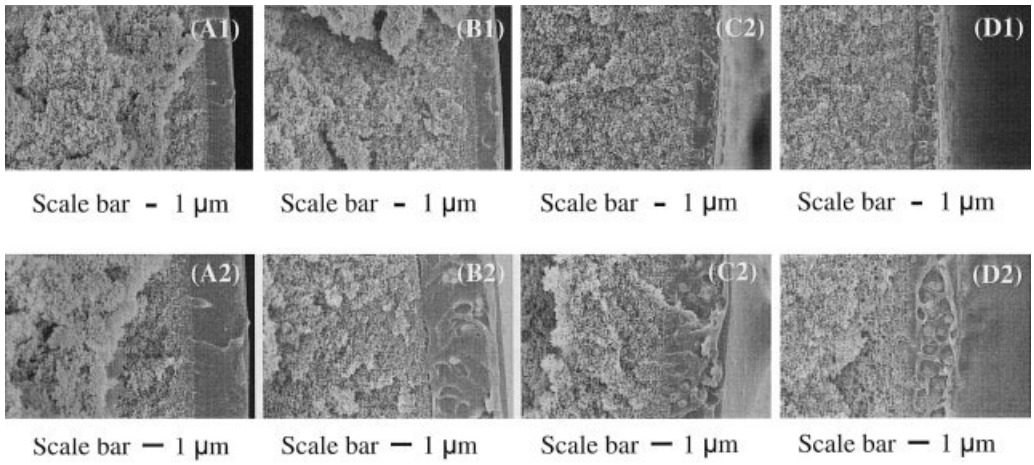

Figure 6. Effect of *p*-xylenediamine solution treatment on the structure of mixed-matrix outer layer.

(A) OL1-D (no zeolite); (B) OL2-D (10 wt % zeolite loading); (C) OL3-D (20 wt % zeolite loading); (D) OL4-D (30 wt % zeolite loading).

tion, the simultaneous attachment of the *p*-xylenediaime to the bulk polymer and particle surface may help the two phases obtain more similar physical properties; consequently, the polymer can wet the particle more easily.

Pure gas permeation properties as a function of posttreatment procedures and zeolite loading

The relationship between selectivity vs. permeance of hollow fibers with the outer layer (~1.5 μm thick) is plotted in Figure 9. These fibers were heat treated at 200°C but without *p*-xylenediamine/methanol presoaking. The performances both before and after the two-step coating are shown in one graph. Before coating, the permeance ranges from 1 to 9 GPU and the highest selectivity is only 1.5 for O_2/N_2 separation, which is significantly inferior to intrinsic property of PSF material.[52,53] After the two-step coating, the permeance is appreciably decreased for all the fibers; however, the selectivity does not necessarily increase uniformly. Module **A** with a permeance of 4 GPU and selectivity of only 1 obtained a selectivity of 6.2 after coating. However, for the other three modules, the selectivity is just around or much lower than 6.2. For module **C**, the selectivities before and after coating are 1 and 4, respectively; for module **D**, they are 1.5 and 2.6, respectively. By comparing with neat PSF/Matrimid® hollow fibers reported in our previous work, the point can be made that selectivity of this mixed-matrix hollow fibers can be improved to be higher than that of neat PSF membrane; the mechanism for improvement will be discussed later.

The assorted morphologies of the outer layer structure in Figure 4 can fundamentally explain the fluctuation in transport performance after the two-step coating. Figure 10 exhibits the morphology of the hollow-fiber cross section before and after coating. Surprisingly, the initial structure with a jagged, irregular morphology and observable polymer–zeolite interface voids becomes completely defect free and smooth after coating. This transformation indicates that the two-step coating materials can effectively fill the voids and pinholes. However,

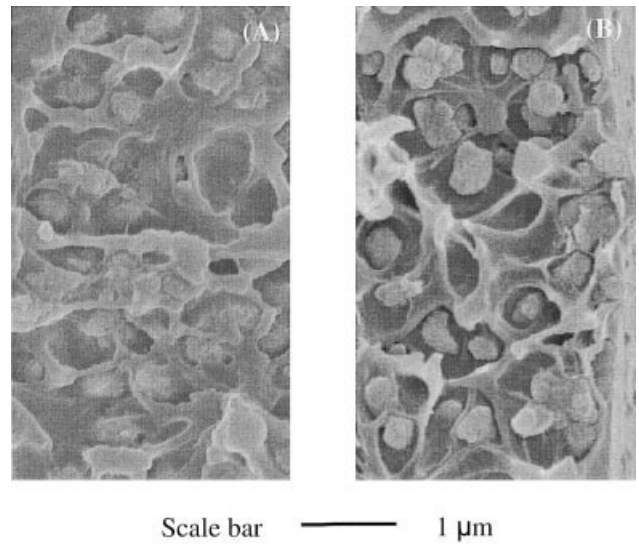

Figure 7. Comparison of the cross section of the outer mixed-matrix layers with (A) and without (B) *p*-xylenediamine/methanol solution treatment.

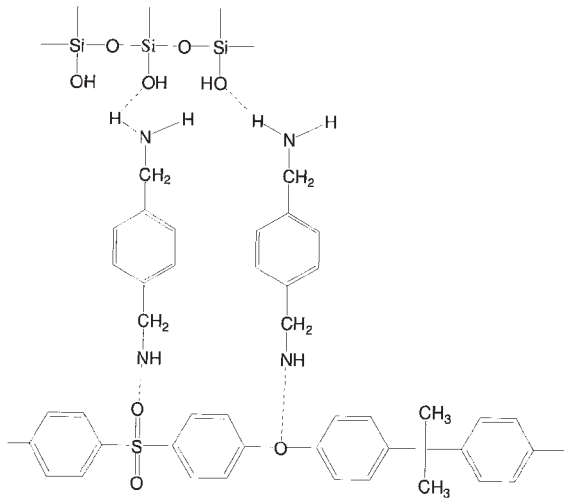

Figure 8. Mechanism of *p*-xylenediamine priming and possible structure.

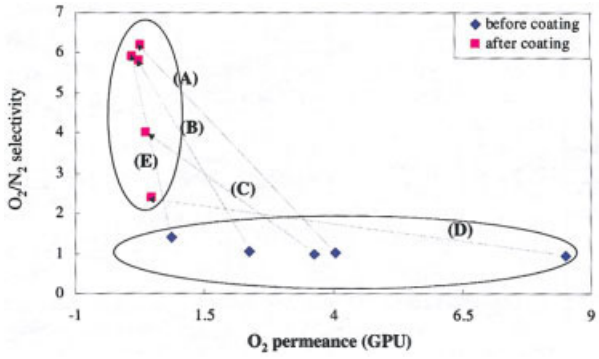

Figure 9. Various separation performances of the mixed-matrix hollow fibers with heat treatment at 200°C (Fiber DL2D).

(A), (B), and (E) selectivity near neat PSF/Matrimid® hollow fiber; (C) and (D) selectivity lower than that of neat PSF/Matrimid® hollow fiber. (A)–(D) 2 h at 200°C; (E) 6 h at 200°C. Testing conditions: 5 atm, 35°C. [Color figure can be viewed in the online issue, which is available at www.interscience.wiley.com]

the gas separation property of the filling material as a third phase in MMM will be involved in the overall performance of the membrane as indicated by Boom[19] and Vu et al.[26] Because silicone rubber has a relatively low selectivity and very high permeability, if interface voids and pinholes are large and exist in great amounts (as shown in Figures 4B and 4C), the coating material (silicon rubber) will dominate as a third phase in the outer layer, and the gas penetrant will go through this bypass instead of the mixed matrix; subsequently, the selectivity cannot be improved (modules C and D in Figure 9). If only a very small portion of defects exists, however, the role of filling/coating material will not overtake the function of the bulk mixed-matrix material (modules A and B in Figure 9). For fiber E with prolonged heat treatment, the permeance was severely

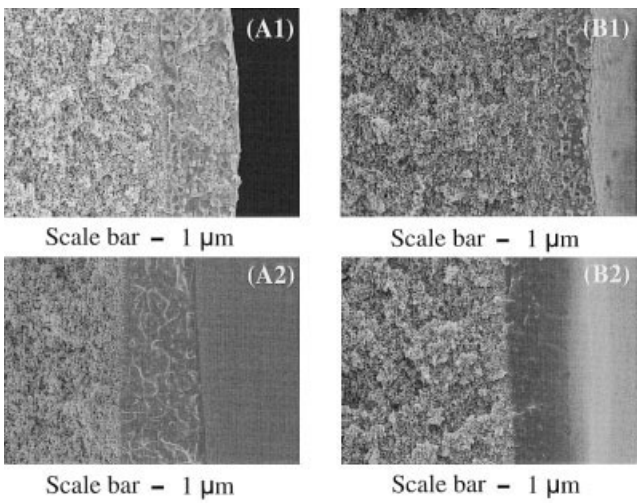

Figure 10. Outer layer cross section morphology before and after coating for the fibers without *p*-xylenediamine/methanol solution soaking.

(A) Fiber DL3C (20 wt % zeolite loading); (B) Fiber DL4D (30 wt % zeolite loading): (1) before coating; (2) after coating.

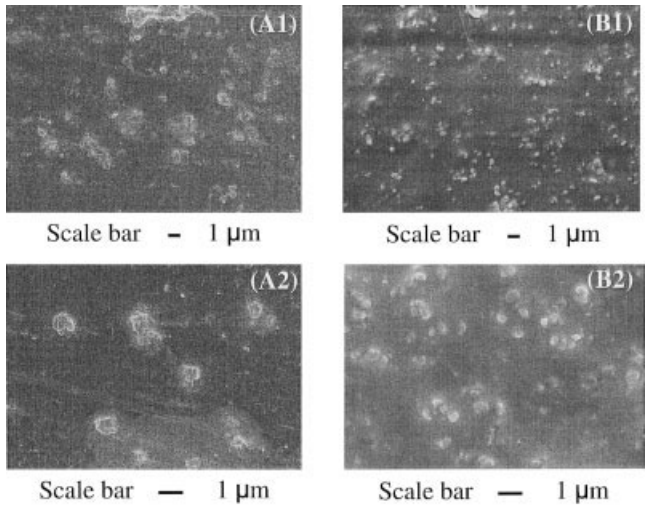

Figure 11. Outer surface morphology of the hollow fibers with and without *p*-xylenediamine /methanol treatment.

(A) Without *p*-xylenediamine/methanol solution treatment for fiber DL3D (20 wt % zeolite loading; (B) with *p*-xylendiamine solution treatment for fiber DL4D (30 wt % zeolite loading).

diminished, probably as a result of the densification of the inner layer at prolonged thermal treatment. The following two subsections will discuss the performance of the hollow fibers with *p*-xylenediamine/methanol treatment.

Hollow Fiber Performance before Coating. As discussed in the previous section, the soaking of hollow fibers in the *p*-xylendiamine/methanol solution will help to achieve better cross-sectional morphology, especially the polymer–zeolite interface. The morphology of the outer surface of the dual-layer hollow fibers is displayed in Figure 11. For fibers without this *p*-xylenediamine/methanol soaking, the particle and polymer phases still have a distinct boundary, as shown in Figures 11A1 and 11A2, whereas by applying both the *p*-xylenediamine/methanol solution soaking and heat treatment, instead the distinct boundary was not observed (Figures 11B1 and 11B2). The selectivity vs. permeance relationship for the uncoated hollow fibers is described in Figure 12. For comparison, the performance for fibers without *p*-xylenediamine/methanol soaking is also plotted. The permeances of the fibers without *p*-xylenediamine/methanol treatment are almost all >1 GPU, whereas selectivities cluster around 1 for both 20 and 30 wt % loading of particles in the polymer matrix. By implementing *p*-xylenediamine/methanol soaking before heat treatment, the permeances of all the fibers are <1 GPU, and selectivity can reach as high as around 3 even without coating to seal some large defects. That the selectivity is much greater than the Knudsen diffusion suggests an appreciably less-defective structure, which might arise from removal of the polymer–particle defects inside the outer layer by *p*-xylenediamine priming.

Hollow Fiber Performance after Two-Step Silicone Rubber Coating. Figures 13 and 14 compare the pure gas permeation data (permeance and selectivity) of the heat-treated dual-layer hollow fibers having a PSF/zeolite beta outer layer with that having a neat PSF outer layer. All the fibers have been coated using the two-step coating as shown in Figure 1. With coating,

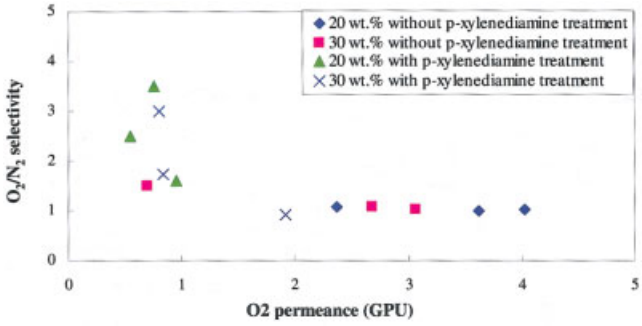

Figure 12. Performance of the mixed-matrix hollow fibers with *p*-xylenediamine/methanol soaking and heat treated at 200°C for 2 h.

Testing conditions: 5 atm, 35°C. [Color figure can be viewed in the online issue, which is available at www.interscience.wiley.com]

the O_2 permeances of the hollow fibers in Figure 13 fall between 0.3 and 0.6 GPU and the permeance of CO_2 in Figure 14 lies between 1.5 and 3 GPU. Generally, the permeance decreases with increasing zeolite loading. This relationship is not strictly obeyed throughout all the loadings, probably because of the trivial differences in the outer selective layer thickness. Because of the relatively thick selective skin, the fluxes of these fibers are low compared to that of commercial membranes. Future investigations will aim to overcome it.

It can also be observed in Figures 13 and 14 that all the fibers show sensible O_2/N_2 and CO_2/CH_4 selectivities; moreover, the fibers with a PSF/beta zeolite outer skin have a substantially improved effective selectivity for these two separations. The fibers with neat PSF outer layer have selectivity $\approx$ 5.6 for O_2/N_2[52,53]; with addition of zeolite beta and increasing its loading to 30 wt %, the selectivity reaches around 7.4 for the fibers. The selectivity of CO_2/CH_4 for fibers with neat PSF outer layer averages 24; after encapsulating zeolite beta particles inside the PSF matrix, the selectivity is improved to around 32 for fibers with 20 wt % of zeolite loading and 39 for 30 wt %. Mixed gas measurement is important for obtaining the true membrane performance in industrial applications.

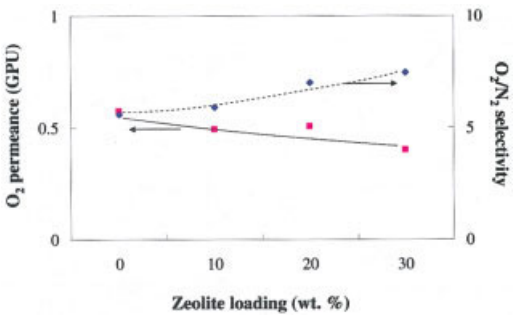

Figure 13. O_2 permeance and O_2/N_2 selectivity of the dual-layer mixed-matrix hollow fibers as a function of zeolite loading after coating with *p*-xylenediamine/methanol soaking and heat treated at 200°C for 2 h.

Testing conditions: 5 atm, 35°C. [Color figure can be viewed in the online issue, which is available at www.interscience.wiley.com]

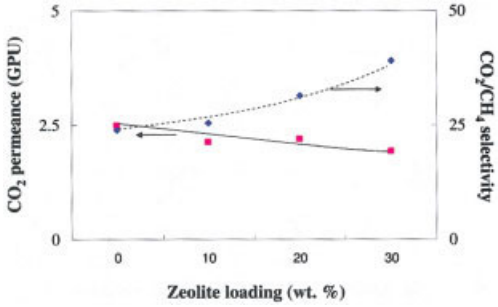

Figure 14. CO_2 permeance and CO_2/CH_4 selectivity of the dual-layer mixed-matrix hollow fibers as a function of zeolite loading after coating with *p*-xylenediamine/methanol soaking and heat treated at 200°C for 2 h.

Testing conditions: 5 atm, 35°C. [Color figure can be viewed in the online issue, which is available at www.interscience.wiley.com]

There may be some differences between pure gas and mixed gas separation results. Possible reasons are the competition in sorption among the penetrants, the concentration polarization, and the nonideal gas behavior. Our previous work[54] on O_2/N_2 and CO_2/CH_4 mixed gas permeation indicated that the mixed-matrix hollow fibers showed a very similar separation property in mixed and pure gas tests. Therefore, these dual-layer hollow-fiber membranes are applicable in industry for gas separation.

The pore size of zeolite beta (on plane $\langle 100 \rangle$: 6.6 $\times$ 6.7Å; on $\langle 001 \rangle$ plane: 5.6 $\times$ 5.6 Å)[55] is larger than the kinetic diameters of all the gases tested. At first glance, selectivity improvement for the two gas pairs contradicts the conventional proposition based on the molecular sieving effects. However, several factors may combine to lead to the selectivity enhancement phenomenon in this study[32,36,37,56,57]: (1) polymer chain rigidification upon the inorganic particle surface and (2) zeolite partial pore blockage. When there is good attachment between the polymer phase and particle or dispersed phase, the presence of dispersed entities can affect the fundamental properties of the polymer matrix. It was proposed by Eisenberg et al.[58] that the multiplet clusters with anchored polymer chains behave as crosslinks in the bulk polymer. In the polymer/inorganic particle mixed-matrix structure, the mobility of a polymer chain in the region directly contacting the particles can be inhibited relative to the rest of the chains in the bulk polymer.[32,57,58] Upon rigidification of polymer chains, the diffusivity of larger gas molecules may be reduced to a greater degree than that of smaller gas molecules.[32,57] Consequently, higher selectivity in this region in the vicinity of the particles may result, which will contribute to the overall performance of the mixed-matrix structure. Moaddeb and Koros[57] found that the O_2/N_2 selectivities for six polymers were significantly improved by bringing the polymer chains in close contact with the impermeable silica particles. The higher selectivities were attributed solely to the restriction of chain segmental mobility, possibly as a result of the adsorption of polymer to the silica surface. In this study, an intimate interfacial packing between the polymer and zeolite beta surface is demonstrated in Figure 7B. The good adhesion is derived from the strong interaction between the two phases with the help of the *p*-xylenediamine. These morphological observations suggest that the polymer chain restriction is very

likely to occur in the vicinity of the zeolites, resulting in higher selectivity.

In the organic/inorganic system, polymer and zeolite adjacent to each other will also affect each other's properties. A significantly important effect is with respect to the partial invasions of polymer chains into the zeolite framework or the partial pore occlusion.[29,37,59-61] In the study reported by Vankelecom et al.,[59] the sorption capacity of polymer/zeolite Y mixed-matrix membrane by experiments was considerably lower than what could be expected theoretically from the properties of the individual polymer and zeolite materials. This drastic change occurring in polymer when zeolite was added was explained by assuming a partial invasion of polymer chains into the zeolite framework and confirmed by the densities of the zeolite-filled membranes as a function of zeolite loading. Li et al.[37] determined that O_2/N_2 selectivity of a PES-5A mixed-matrix membrane was higher than that of a PES-4A mixed-matrix membrane. Their explanation for this interesting observation is that the pore opening of 4.5 Å in zeolite 5A was reduced to such a degree by the partial pore blockage as to discriminate different molecules more accurately. It can also be reasonably expected that the 12-ring pores of zeolite beta may be occluded by the surrounding materials, thus obtaining a higher separation property. Both the polymer chain inhibition and zeolite pore blockage are factors that can lead to the lower-than-predicted permeability. This may explain why the permeances in Figures 13 and 14 follow the decreasing trends with increasing zeolite loading, if the thickness of the selective layer is assumed to be the same.

Further comparison of Figures 13 and 14 indicates that the increment in CO_2/CH_4 selectivity is more impressive than that in O_2/N_2. This difference may be explained by a larger size difference between CO_2 and CH_4 molecules than that between O_2 and N_2 molecules. The kinetic diameters of O_2 and N_2 are 3.46 and 3.64 Å, respectively, and their difference is only 0.18 Å. On the other hand, the kinetic diameters of CO_2 and CH_4 are 3.3 and 3.8 Å, respectively. In addition, the preferential adsoption of CO_2 in the zeolite with monovalent alkali cations or the affinity between CO_2 and zeolite may provide higher sorption selectivity in these mixed-matrix structures than in the neat PSF structure.[20,59,62,63]

Conclusions

For the first time, a novel *p*-xylenediamine/methanol treatment has been introduced in the fabrication of high-performance mixed-matrix hollow fibers for gas separation. Based on the gas separation results and characterizations in this research, the following conclusions can be made:

(1) The morphology of the as-spun hollow fibers shows that the particles located near the outer surface of the hollow fibers may form some partially defect free mixed-matrix structure with the surrounding polymer arising from the instantaneously solidified polymer phase. However, a continuous defect-free skin structure has not been obtained because of the defects existing in the polymer matrix and the detachment of polymer chains from the particle surface during posttreatment.

(2) Thermal treatment with *p*-xylenediamine/methanol solution soaking as a pretreatment produces a more uniform and less defective mixed-matrix structure in the outer mixed-matrix layer of the dual-layer hollow fibers. Some fibers even obtain selectivity much higher than Knudsen diffusion even without silicone rubber coating, which indicates the significantly reduced amount of defects.

(3) After the two-step silicone rubber coating, the mixed-matrix hollow fibers with *p*-xylenediamine/methanol solution soaking and thermal treatment show selectivity much higher than that of neat PSF/Matrimid® hollow fibers. Possible causes for the improvement are physical crosslinking/rigidification of polymer chains induced by zeolites, partial pore blockage of zeolite pores, and the possible interaction between the gas penetrant and zeolite internal surfaces.

In this study, the productivity of the mixed-matrix hollow fibers is relatively low because of the thick skin (1.5 μm). The focus of our future work will be to reduce the mixed-matrix skin layer thickness. To fulfill this purpose, synthesis of considerably smaller zeolite particles, prevention of particle aggregation, and compatibilization of particle and polymer are of utmost importance; investigation on the relationship between particle size and outer layer thickness will also be useful. In addition, implementation of the fibers at a correct scale will also be part of our future work to make these fibers industrially applicable.

Acknowledgments

This work was financially supported by UOP LLC and National University of Singapore Grants R-279-000-140-592, R-279-000-140-112, and R-279-000-184-112. Special appreciation is extended to Dr. Zhen Huang for the provision of beta zeolite and to Yi Li, Dr. Pei Shi Tin, and Youchang Xiao for offering helpful suggestions concerning permeation cell modification and hollow-fiber spinning.

Literature Cited

1. Paul DR, Yampol'skii YP. *Polymeric Gas Separation Membranes*. Boca Raton, FL: CRC Press; 1994.
2. Pinnau I, Freeman BD. *Membrane Formation and Modification*. Washington, DC: American Chemical Society; 1990.
3. Kulprathipanja S, Neuzil RW, Li NN. *Gas Separation by Means of Mixed Matrix Membranes*. U.S. Patent 4 740 219; 1988.
4. Vu DQ, Koros WJ, Miller SJ. Mixed matrix membranes using carbon molecular sieves. I. Preparation and experimental results. *J Membr Sci*. 2003;211:311–334.
5. Merkel TC, Freeman BD, Spontak RJ, He Z, Pinnau I, Meakin P, Hill AJ. Ultrapermeable, reverse-selective nanocomposite membranes. *Science*. 2002;296:519–522.
6. Tin PS, Chung TS, Jiang LY, Kulprathipanja S. Carbon–zeolite composite membranes for gas separation. *Carbon*. 2005;43:2025–2027.
7. Triebe RW, Tezel FH, Khulbe KC. Adsorption of methane, ethane and ethylene on molecular sieve zeolites. *Gas Sep Purif*. 1996;10:81–84.
8. Hutson ND, Rege SU, Yang RT. Mixed cation zeolites: Li_xAg_y-X as a superior adsorbent for air separation. *AIChE J*. 1999;45:724–734.
9. Singh A, Koros WJ. Significance of entropic selectivity for advanced gas separation membranes. *Ind Eng Chem Res*. 1996;35:1231–1234.
10. te Hennepe HJC, Bargeman D, Mulder MHV, Smolders CA. Zeolite-filled silicone rubber membranes. Part 1. Membrane preparation and pervaporation results. *J Membr Sci*. 1987;35:39–55.
11. Goldman M, Frankel D, Levin G. A zeolite/polymer membrane for the separation of ethanol water azeotrope. *J Appl Polym Sci*. 1989;37:1791–1800.
12. Jia M, Peinemann KV, Behling RD. Molecular sieving effect of the zeolite-filled silicone rubber membranes in gas permeation. *J Membr Sci*. 1991;57:289–292.
13. Bartels-Caspers C, Tusel-Langer E, Lichtenthaler RN. Sorption isotherms of alcohols in zeolite-filled silicon rubber and in PVA-composite membranes. *J Membr Sci*. 1992;70:75–83.
14. Guan HM, Chung TS. Poly(vinyl alcohol) multilayer mixed matrix membranes for the dehydration of ethanol–water mixture. *J Membr Sci*. 2006;268:113–122.

15. Paul DR. Effect of immobilizing adsorption on the diffusion time lag. *J Polym Sci Part A-2*. 1969;7:1811–1824.
16. Paul DR. The diffusion time lag in polymer membranes containing adsorptive fillers. *J Polym Sci Symp*. 1973;41:79–93.
17. Kulprathipanja S, Neuzil RW, Li NN. *Separation of Gases by Means of Mixed Matrix Membranes*. U.S. Patent 5 127 925; 1992.
18. Jia MD, Peinemann KV, Behling RD. Preparation and characterization of thin-film zeolite PDMS composite membranes. *J Membr Sci*. 1992; 73:119–128.
19. Boom JP. *Transport through Zeolite Filled Polymeric Membranes*. PhD Thesis. Enschede, The Netherlands: The University of Twente; 1994.
20. Duval JM. *Adsorbant Filled Polymeric Membranes*. PhD Thesis. Enschede, The Netherlands: The University of Twente; 1994.
21. Vankelecom IFJ, Van den Broeck S, Merckx E, Geerts H, Grobet P, Uytterhoeven JB. Silylation to improve incorporation of zeolites in polyimide films. *J Phys Chem*. 1996;100:3753–3758.
22. Guiver MD, Le Thi HN, Robertson GP. *Composite Gas Separation Membranes*. U.S. Patent 6 605 140, 2002.
23. Rojey A, Deschamps A, Grehier A, Robert E. *Separating Gases Using Zeolite-Containing Composite Membranes*. U.S. Patent 4 925 459; 1990.
24. Kulkarni SS, Hasse DJ, Corbin DR, Patel AN. *Gas Separation Membrane with Organosilicon-Treated Molecular Sieve*. U.S. Patent 6 508 860; 2003.
25. Vu DQ, Koros WJ, Miller SJ. Effect of condensable impurity in CO_2/CH_4 gas feeds on performance of mixed matrix membranes using carbon molecular sieves. *J Membr Sci*. 2003;221:233–239.
26. Vu DQ, Koros WJ, Miller SJ. Mixed matrix membranes using carbon molecular sieves. II. Modeling and permeation behavior. *J Membr Sci*. 2003;211:335–348.
27. Gur TM. Permselectivity of zeolite filled polysulfone gas separation membranes. *J Membr Sci*. 1994;93:283–289.
28. Suer MG, Bac M, Yilmza L. Gas permeation characteristics of polymer–zeolite mixed matrix membranes. *J Membr Sci*. 1994;91:77–86.
29. Mahajan R. *Formation, Characterization and Modeling of Mixed Matrix Membrane Materials*. PhD Thesis. Austin, TX: The University of Texas; 1998.
30. Zimmerman CM, Singh A, Koros WJ. Tailoring mixed matrix composite membranes for gas separations. *J Membr Sci*. 1997;137:145–154.
31. Yong HH, Park HC, Kang YS, Won J, Kim WN. Zeolite-filled polyimide membrane containing 2,4,6-triaminopyrimidine. *J Membr Sci*. 2001;188:151–163.
32. Chan SS, Chung TS, Wang R, Lu Z, He C. Characterization of permeability and sorption in Matrimid/C_{60} mixed matrix membranes. *J Membr Sci*. 2002;218:1–9.
33. Wang H, Holmberg BA, Yan Y. Homogeneous polymer–zeolites nanocomposite membranes by incorporating dispersible template-removed zeolite nanoparticles. *J Mater Chem*. 2002;12:3640–3643.
34. Pechar TW, Tspatsis M, Marand E, Davis R. Preparation and characterization of a glassy fluorinated polyimide zeolite-mixed matrix membrane. *Desalination*. 2002;146:3–9.
35. Anson M, Marchese J, Garis E, Ochoa N, Pagliero C. ABS copolymer-activated carbon mixed matrix membranes for CO_2/CH_4 separation. *J Membr Sci*. 2004;243:19–28.
36. Moore TT, Koros WJ. Non-ideal effects in organic–inorganic materials for separation membranes. *J Mol Struct*. 2005;739:87–97.
37. Li Y, Chung TS, Cao C, Kulprathipanja S. The effects of polymer chain rigidification, zeolite pore size and pore blockage on polyethersulfone (PES)–zeolite A mixed matrix membranes. *J Membr Sci*. 2005;260:45–55.
38. Jiang LY, Chung TS, Cao C, Huang Z, Kulprathipanja S. Fundamental understanding of nano-sized zeolite distribution in the formation of the mixed matrix single- and dual-layer asymmetric hollow fiber membranes. *J Membr Sci*. 2005;252:89–100.
39. Jiang LY, Chung TS, Kulprathipanja S. An investigation to revitalize the separation performance of hollow fibers with a thin mixed matrix composite skin for gas separation. *J Membr Sci*. 2006;276:113–125.
40. Li Y, Chung T-S, Huang Z, Kulprathipanja S. Dual-layer polyethersulfone (PES)/BTDA-TDI/MDI co-polyimide (P84) hollow fiber membranes with a submicron PES–zeolite beta mixed matrix dense-selective layer for gas separation. *J Membr Sci*. 2006;277:28–37. Available online 22 November 2005.
41. Miller SJ, Munson CL, Kulkarni SS, Hasse DJ. *Purification of p-Xylene Using Composite Mixed Matrix Membranes*. U.S. Patent 6 500 233; 2002.
42. Ekiner OM, Kulkarni SS. *Process for Making Hollow Fiber Mixed Matrix Membranes*. U.S. Patent 6 663 805; 2003.
43. Koros WJ, Wallace D, Wind JD, Miller SJ, Bickel CS, Vu DQ. *Crosslinked and Crosslinkable Hollow Fiber Mixed Matrix Membrane and Method of Making Same*. U.S. Patent 6 755 900; 2004.
44. Yanagimoto T. *Manufacture of Ultrafiltration Membranes*. Japanese Patent 62019205; 1987.
45. Jiang LY, Chung TS, Li DF, Cao C, Kulprathipanja S. Fabrication of Matrimid/polyethersulfone dual-layer hollow fiber membranes for gas separation. *J Membr Sci*. 2004;240:91–103.
46. Li DF, Chung TS, Wang R. Morphological aspects and structure control of dual-layer asymmetric hollow fiber membranes formed by a simultaneous co-extrusion approach. *J Membr Sci*. 2004;243;155–175.
47. Li Y, Cao C, Chung TS, Pramoda KP. Fabrication of dual-layer polyethersulfone (PES) hollow fiber membranes with an ultrathin dense selective layer for gas separation. *J Membr Sci*. 2004;245:53–60.
48. Ekiner OM, Hayes RA, Manos P. *Reactive Post Treatment for Gas Separation Membranes*. U.S. Patent 5 091 216; 1992.
49. Bikson B, Nelson JK. *Composite Membranes and Their Manufacture and Use*. U.S. Patent 4 826 599; 1989.
50. Gollan AZ. *Anisotropic Membranes for Gas Separation*. U.S. Patent 4 681 605; 1987.
51. Chung TS. A review of microporous composite polymeric membrane technology for air-separation. *Polym Polym Comp*. 1996;4:269–283.
52. Mohr JM, Paul DR, Pinnau I, Koros WJ. Surface fluorination of polysulfone asymmetric membranes and films. *J Membr Sci*. 1991;56: 77–98.
53. Aitken CL, Koros WJ, Paul DR. Gas transport properties of biphenol polysulfones. *Macromolecules*. 1992;25:3651–3658.
54. Li Y, Jiang LY, Chung T-S. A new testing system to determine the O_2/N_2 mixed-gas permeation through hollow-fiber membranes with an oxygen analyzer. *Ind Eng Chem Res*. 2006;45:871–874.
55. Meier WM, Olson DH. *Altas of Zeolite Structure Types*. 3rd Edition. London, UK: Butterworth-Heinemann; 1992.
56. Li Y, Guan H-M, Chung T-S, Kulprathipanja S. Effects of novel silane modification of zeolite surface on polymer chain rigidification and partial pore blockage in polyethersulfone (PES)–zeolite A mixed matrix membranes. *J Membr Sci*. 2006;1275:17–28.
57. Moaddeb M, Koros WJ. Gas transport properties of thin polymeric membranes in the presence of silicon dioxide particles. *J Membr Sci*. 1997;125:143–163.
58. Eisenberg A, Hird B, Moore RB. A new multiplet-cluster model for the morphology of random ionomers. *Macromolecules*. 1990;23: 4098–4107.
59. Vankelecom IFJ, Scheppers E, Heus R, Uytterhoeven JB. Parameters influencing zeolite incorporation in PDMS membranes. *J Phys Chem*. 1994;98:12390–12396.
60. Vankelecom IFJ, Merckx E, Luts M, Uytterhoeven JB. Incorporation of zeolite in polyimide membranes. *J Phys Chem*. 1995;99:13187–13192.
61. Al-Ghamdi AMS, Mark JE. Zeolites as reinforcing fillers in an elastomer. *Polym Bull*. 1988;20:537–542.
62. Hasegawa Y, Watanabe K, Kusakabe K, Morooka S. Influence of alkali cations on permeation properties on Y-type zeolite membranes. Short communication. *J Membr Sci*. 2002;208:415–418.
63. Li P, Tezel FH. Adsorption separation with β-zeolite for N_2, O_2, CO_2 and CH_4 by concentration pulse chromatography.

Manuscript received Oct. 22, 2005, and revision received May 3, 2006.